



Original Article

Induction of Apoptosis and Inhibition of Breast Cancer Cell Growth and Multicellular Tumor Spheroids by Paclitaxel Combined Curcumin-loaded PLA-TPGS-based Nanoparticles

Nguyen Duc Tu^{1,2,*}, Tran Phan Anh^{1,3}, Ha Phuong Thu⁴, Nguyen Hoai Nam⁴,
Nguyen Xuan Phuc⁴, Hoang Thi My Nhung¹

¹VNU University of Science, 334 Nguyen Trai, Thanh Xuan, Hanoi, Vietnam

²Vinmec Healthcare System, 458 Minh Khai, Hai Ba Trung, Hanoi, Vietnam

³The People's Police Academy, Co Nhue 2, Bac Tu Liem, Hanoi, Vietnam

⁴Vietnam Academy of Science and Technology, 18 Hoang Quoc Viet, Hanoi, Vietnam

Received 28 July 2021

Revised 31 August 2021; Accepted 03 September 2021

Abstract: Paclitaxel and curcumin have been reported as anti-cancer compounds. Here, we presented a novel combination of paclitaxel and curcumin-loaded PLA-TPGS (PTX-Cur/PLA-TPGS) nanoparticles prepared by a modified solvent extraction/evaporation technique. These nanoparticles were well distributed and stable in water. This combination of paclitaxel and curcumin gave a higher efficiency of both drugs in cytotoxicity, induced apoptosis, and effect on cell cycles of KPL4 cell line in comparison with the use of paclitaxel or curcumin alone or even a normal mixture of these two compounds. Furthermore, PTX-Cur/PLA-TPGS nanoparticles exhibited a powerful ability in preventing MCF7 spheroids growth. Interestingly, curcumin also functioned as both a drug and a label. Based on the autofluorescence of curcumin, the absorption of PTX-Cur/PLA-TPGS nanoparticles into MCF7 spheroids could be followed and calculated. These results suggest that the nanoparticle-combination may provide a promising multifunctional delivery system for anti-cancer drugs.

Keywords: Paclitaxel, curcumin, PLA-TPGS nanoparticles, breast cancer, apoptosis, multicellular tumor spheroid.

1. Introduction

Breast cancer is the most frequent cancer affecting women worldwide with the fifth mortality rate. In 2020, about 684,996 people

died of this cancer, comprised 6.9% of cancer deaths [1]. Paclitaxel is a major anti-cancer drug isolated from the bark of *Taxus brevifolia*, and its anti-cancer effect has long been widely applied in cancer chemotherapy. Paclitaxel interferes with the dynamic instability of microtubule and as a result, prevents the transition of mitotic cells from metaphase to anaphase. Cells are arrested at G2/M and finally

* Corresponding author.

E-mail address: v.tund5@vinmec.com

<https://doi.org/10.25073/2588-1140/vnunst.5284>

go to apoptosis. This drug is approved for its use as second-line treatment of ovarian and breast cancers [2]. However, as with other chemotherapy drugs, paclitaxel causes side effects, especially in myelotoxicity and neurotoxicity [3]. The combination of paclitaxel with many other anti-cancer drugs to alter its pharmacokinetics, enhance its efficiency, and reduce the side effect has been studied [4].

Curcumin is the major curcuminoids extract from the root of turmeric, and is known for its anti-oxidant, anti-inflammatory effect [5] and antiseptic activity. Curcumin has been used widely in many Asian countries as a traditional medicine and food. It has been reported about the safety of this compound in daily life use in certain countries [6]. More recently, Curcumin has been found to possess anti-cancer activities via its effects on mutagenesis, oncogene expression, cell cycle regulation, apoptosis, tumorigenesis and metastasis [7]. Curcumin has an inhibitory effect on NF- κ B and AP-1 activation; down-regulation of cyclin D and MMP-1 transcription [8]. Besides that, Curcumin with its autofluorescence can be used for labeling the drug complex [9].

That both curcumin and paclitaxel are highly insoluble in water leads to low absorption rate. One of the solutions is to encapsulate paclitaxel or curcumin in polymeric nanoparticle [10].

It was found that poly(lactide)-vitamin E TPGS (PLA-TPGS) copolymer can greatly increase the drug encapsulation efficiency and PLA-TPGS-based nanoparticle formulation avoids using toxic adjuvant Cremophor EL. The nanoparticles are also very stable at room temperature [11]. In addition, PLA-TPGS micelles co-loaded Curcumin and paclitaxel showed a dual-function nano system for theranostics [12]. This study concentrated on exploring the ability of Curcumin as a label compound for cellular uptake and penetrating in the tumor spheroids [12].

The combination of drugs with different anti-cancer activities could bring more advantages in cancer treatment. In this way, it would make synergistic therapeutic effects in

killing cancer cells. Ganta has reported the effectiveness in enhancing the cytotoxicity in wild-type and resistant cells by promoting the apoptotic response by co-administration of paclitaxel and curcumin in single drug delivery systems [13]. However, it is difficult to control the drug release behavior of each drug at therapeutic sites. Therefore, drug delivery systems that simultaneously load drugs have been researched with the aim of solving that challenge [14]. Besides, Kim et al., [15] reported about the ability of biodegradable polymeric nanoparticles with paclitaxel and curcumin against breast carcinoma in mice.

In this study, (PTX combined Cur)-loaded PLA-TPGS nanoparticle is the main subject. The cytotoxicity and the ability to induce the apoptosis process of cancer cells of the complex were evaluated. Especially, we investigated the ability of this nanoparticulate complex in inhibition of MCF7 spheroid growth. Our results showed that Paclitaxel and Curcumin encapsulated in PLA-TPGS nanoparticle effectively inhibited breast cancer cells in both 2D and 3D culture and increased the nanoparticle-induced apoptosis.

2. Methodology

2.1. Materials

Paclitaxel (PTX) was purchased from Dabur Pharma Limited, India. Curcumin (Cur) was purchased from Mumbai, India.

PTX-loaded poly(lactide)-vitamin E TPGS (PLA-TPGS) copolymer (PTX/PLA-TPGS), Curcumin-loaded PLA-TPGS, and PTX combined Cur-loaded PLA-TPGS nanoparticles (PTX-Cur/PLA-TPGS) were synthesized and supplied from the Institute of Material Science. These nanoparticles were well characterized with the round shape, and size ranged from 50 - 120 nm [12, 16].

2.2. Cell Culture

The two human breast cancer cell lines: MCF7 and KPL4 were grown on Dulbecco's modified Eagle's 1 g/l of Glucose in a tissue culture dish. Media were supplemented with 10% (v/v) fetal

bovine serum, penicillin-streptomycin 100 IU/ml, L-glutamine 2 mM. Cells were grown in a humidified chamber in the presence of 5% CO₂, at 37 °C. Cell culture materials were supplied from Invitrogen.

Cell proliferation assays were conducted in a 96-well plate, in normal growth conditions. Assays were run in four replicates. After 72 h of incubation with the compounds, cell viability was estimated by using MTS kit (Promega).

2.3. Morphology Analysis of Apoptosis

For morphology analysis of apoptosis, compound-treated cells were grown on 14-mm-diameter glass coverslips (Knittel gläser) for 24 hours at 37 °C in 4% (w/w) paraformaldehyde, 2% (w/w) sucrose and then permeabilized with 0.2% Triton X-100 in PBS for 5 min. DNA was visualized by staining with 0.1 μM Hoechst (Invitrogen). Images were collected with a ZEISS 510 Laser Scanning Confocal apparatus with a 40x or 63x immersion oil objective.

2.4. Analysis of Apoptosis by Propidium Iodide Staining and Flow Cytometry

We used the method proposed by Riccardi & Nicoletti [17]. Briefly, 2×10⁶ cells were harvested and fixed in 70% (v/v) cold ethanol for 30 min. After washing 3 times by PBS, remove the supernatant and resuspend cells in 1 ml of DNA staining solution (PBS containing 2% PI (wt/v) and 2% DNase free RNase (wt/v)). Cells were incubated with DNA staining solution for 30 minutes at room temperature and in the dark. Cells were then analyzed by FACS Canto II, used 488-nm laser for excitation. Red fluorescence of PI (> 600 nm) was measured with side scatter (SSC) and forward scatter (FSC). At least 20,000 events were collected. Residual debris was gated - out using multilabel microbeads with size of 2 and 3 μm. Apoptotic cells are characterized by DNA fragmentation and bound to PI. When analyzing by flow cytometry, these cells display a broad hypodiploid sub-G1 peak, separately from the diploid peak (G0-G1) and pluriploid peak (cells with a ploidy superior to 2N).

2.5. Multicellular Tumor Spheroid (MCTS) Culture

MCF7 cell line is reported to have high ability to create spheroids when using hanging drop method [18] with a slight modification. 15 μl medium containing 5,000 cells was added to each circle on the inverted - cover of 96-well plate for making one spheroid. Then the cover was placed upside down on the plate and coated with sterile agarose 1.5% (wt/v) containing 200 μl complete medium. After 48 hours of incubation in a humidified chamber in the presence of 5% CO₂, at 37 °C, spheroids were transferred from the cover into each well of the agarose-coated plate and further cultivated in fresh growth medium.

2.6. MCTS Culture Kinetics

Images of MCTS in each well were taken by Axiovert 40CFL microscope (Zeiss) with Powershot G9 camera. These images were analyzed using Axio version 4.5 (Zeiss) to determine MCTS diameter. The volume of each spheroid was calculated by the formula for the volume of a sphere [19]: $V = 4/3 \pi r^3$.

2.7. Cellular Uptake and Immunofluorescent Imaging of Whole-mount Spheroids

MCF7 spheroids grown on agarose-coated 96-well plate were cultured in the presence of the combination at the concentration of 0.09 μM paclitaxel and 0.43 μM curcumin. After 2 h, 8 h and 24 h of incubation, spheroids were fixed in 3.7% formaldehyde solution for 2 h at room temperature. Samples were rinsed in PBS and mounted in 80% glycerol in the chambers of a gasketed microscope slide, and left to clear for at least 4 h. Imaging was achieved using a LSM510 confocal microscopy system based on the autofluorescence of Curcumin. Negative controls were processed without incubation of any compounds.

2.8. Statistical Analysis

GraphPad Prism 5 was used to calculate the IC50 values and make dose-response curves. One-way ANOVA was used to compare the IC50 values of the compounds. A p-value < 0.05 represented statistically significant difference.

3. Results and Discussion

3.1. Cytotoxicity of PTX-Cur/PLA-TPGS

We have checked the cytotoxicity of compounds: PTX, Cur, PTX/PLA-TPGS, Cur/PLA-TPGS, PTX-Cur (normal mixture of paclitaxel and curcumin with the corresponding concentrations) and PTX-Cur/PLA-TPGS on two breast cancer cell lines - KPL4 and MCF7 cells. The aim of this experiment was to investigate whether there is a synergism between PTX and Cur in normal mixture of two compounds; and, more importantly, is there an increase in synergism when the compounds are co-coated with PLA-TPGS. The MTS assay, the very efficient method for screening anti-proliferating compounds, was used to determine the cell viability in the presence of four compounds with different concentration range from 8.3 nM to 0.625 μ M of paclitaxel and 0.05 to 2.9 μ M of curcumin. The concentrations of paclitaxel and curcumin were similar in Cur, PTX-Cur and PTX-Cur/PLA-TPGS. At the highest dose tested, 0.625 μ M for paclitaxel (in PTX, PTX-Cur and PTX-Cur/PLA-TPGS) and 2.9 μ M for Cur, the viability (%) of cells was low, with around 40%. Since both of PTX and Cur are reported as being cytotoxic at the high dose, it is difficult to see any effect difference on cell viability. However, at the lower doses, there is a big change in the cell viability between the 4 compounds. Cur up to 1.45 μ M exhibited no significant effect on cell viability whereas paclitaxel was highly toxic. The obtained results revealed that PTX alone induced much less cytotoxicity in comparison with the combination of paclitaxel and curcumin in PTX-Cur and PTX-Cur/PLA-TPGS. For example, in KPL4 cells, PTX at 0.3 μ M induced about 23.5% cytotoxicity while the combination of 0.15 μ M paclitaxel and 0.72 μ M curcumin induced 35% cytotoxicity in PTX-Cur and 47% in PTX-Cur/PLA-TPGS (Figure 1). Moreover, PTX-Cur/PLA-TPGS nanoparticles had better effect in inhibition of breast cancer cell growth than PTX/PLA-TPGA and Cur/PLA-TPGS alone (Table 1). The IC50 value of PTX-Cur/PLA-TPGS nanoparticles

was much lower than the other compounds (Table 1). The enhanced effect of the combination between paclitaxel and curcumin on cell viability was proved before by Smitha et al., [13, 20].

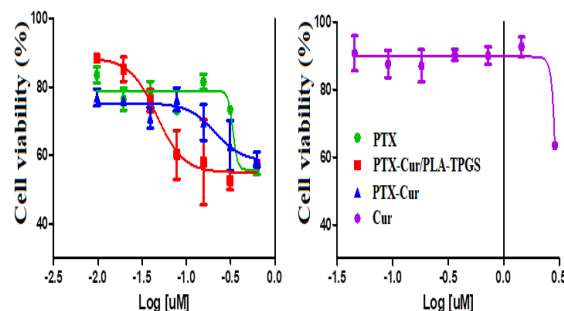


Figure 1. Dose-response curves of PTX, Cur, PTX-Cur and PTX-Cur/PLA-TPGS for KPL4 cell growth. Error bars represent the standard deviation of four replicates.

Our results showed that this combination in nanoparticulate formulation with PLA-TPGS coating increased even much more the cytotoxicity of the two compounds. We would emphasize that only the nanoparticles can be dissolved in water, while the PTX and Cur alone must be dissolved in DMSO. Water solubility is necessary for any drug that will be used for human diseases [21]. Even in water, PTX-Cur/PLA-TPGS showed significant advantages in inhibiting cancer cell proliferation compared to PTX or PTX-Cur in DMSO solution ($p < 0.05$).

Table 1. IC50 values of compounds on MCF7 and KPL4 cell lines

Compounds	IC50 on MCF7 (μ M) (\pm SD)	IC50 on KPL4 (μ M) (\pm SD)
PTX	4.895 \pm 0.536	2.2 \pm 0.08
Cur	43.722 \pm 7.718	17.96 \pm 3.4
PTX/PLA-TPGS	1.093 \pm 0.173	
Cur/PLA-TPGS	23.07 \pm 2.17	
PTX-Cur	5.210 \pm 0.541	1.8 \pm 0.2
PTX-Cur/PLA-TPGS	0.744 \pm 0.156*	0.4 \pm 0.05*
* $p < 0.05$		

3.2. PTX-CUR/PLA-TPGS Induced Apoptosis in Breast Cancer Cells

Most chemotherapeutic anti-cancer drugs used in the clinic today include agents that target the cell cycle in order to inhibit the hyper-proliferation state of tumor cells and subsequently, to induce apoptosis, which is the desired outcome of chemotherapy. Checking the ability of PTX-Cur/PLA-TPGS in increasing PTX or Cur-induced apoptosis is one of the major aims of our work. When staining KPL4 cells with Hoescht, a nucleotide-binding fluorescence dye, we observed that the morphology of the cell's nucleus was perturbed in treated cells. In the control without treatment, most of the cellular nuclei were round and similar in size whereas in PTX or PTX and Cur combination - treated cells, chromatin condensation and DNA fragmentation were observed (Figure 2A). We used a flow cytometry method to determine the percentage of apoptotic cells following administration of either PTX, PTX-Cur, Cur or PTX-Cur/PLA-TPGS at the same concentration (0.36 μM for paclitaxel and 1.68 μM for curcumin) for 48 hours. Based on the fact that in cell culture condition, apoptotic cells can become necrotic if allowed to proceed for a long time because of lacking professional phagocytes that are responsible for clearing apoptotic bodies in vivo [22]; we always checked morphology of cells and cellular nuclear by immunofluorescence from time to time. Cells were harvested only when we observed the DNA fragmentation and cells still stayed in the complete membrane. As shown in Figure 2B, apoptotic nuclear appeared as a "sub-G1" peak (red peak). The percentage of apoptotic nuclear is highest in PTX-Cur/PLA-TPGS (37%), nearly 3 times more than in PTX and PTX-Cur (13% and 13.5%, relatively). In Cur treated cells and control cells, these percentages are similar (3.5% and 3.4%, respectively). Obviously, the nanoparticulate formulation increased the apoptosis in KPL4 cells. The

Figure also presents the effect of paclitaxel on cell cycle. In the presence of either PTX or PTX-Cur, most of cells increased their DNA content, with the percentages of diploid nuclei were 70.6% and 76.4%, respectively, whereas in the control, most of cells stayed in G1 phase (66.4%), and a small part of them (27.2%) were in G2/M phase as diploid peak. Because paclitaxel inhibits the depolymerization of microtubules, it causes mitotic arrest [2].

Cells in the presence of paclitaxel can double their DNA but cannot divide during the M phase. Previous studies on paclitaxel have shown that, treated cells with low concentrations of the drug can firstly cause mitotic slippage. This means cells escape the mitotic checkpoint and turn back to the G1 phase without nuclear dividing. Some of the cells die because of apoptosis, but other cells can continue to the next M phase with the second time of doubling the DNA content. After two rounds of mitotic slippage, most of the cells will go to apoptosis [23]. Cells treated with PTX-Cur/PLA-TPGS spent less time in the G2/M phase or diploid G1 (51%) but more in apoptosis. That means PTX-Cur/PLA-TPGS with the equivalent concentration not only increased the apoptosis but also induced this process to happen earlier than PTX and PTX-Cur.

3.3. PTX+Cur/PLA-TPGS Inhibited MCF7 Spheroid Growth

Multicellular tumor spheroid culture systems show intermediate complexity reflecting particular aspects of tumor tissues including multilayer cell systems [14, 19]. Any compound that showed efficient inhibition of spheroid growth would be a candidate for anti-cancer drug. That is the reason we carried out the experiment on MCF7 spheroid to check the anti-spheroid growth activity of PTX-Cur/PLA-TPGS and to compare it to commercial PTX. The compounds were added to MCF7 spheroids on day 3 of culturing with concentrations ranged from 0.0037 μM to 2.3 μM of paclitaxel. We

observed that all of the treated spheroids decreased in size compared to the control and that PTX-Cur/PLA-TPGS had greater effect on inhibiting MCF7 spheroid growth than PTX alone. After just one day of incubation, both compounds showed an effect on the morphology of spheroids. Some cells of the outer layer - the highest proliferated part in spheroid structure - became more loosely bound together. It is more clearly on day 4 of

treatment when cells in outer layer begin to die and the spheroids lost their tightly-linked border (Figure 3A). By attacking the proliferating cells, the nanoparticles inhibited the growth of spheroids. There was no increase in size or volume of spheroids treated with any dose of PTX-Cur/PLA-TPGS even from day 1 of treatment, whereas the controls were frequently larger (Figure 3A).

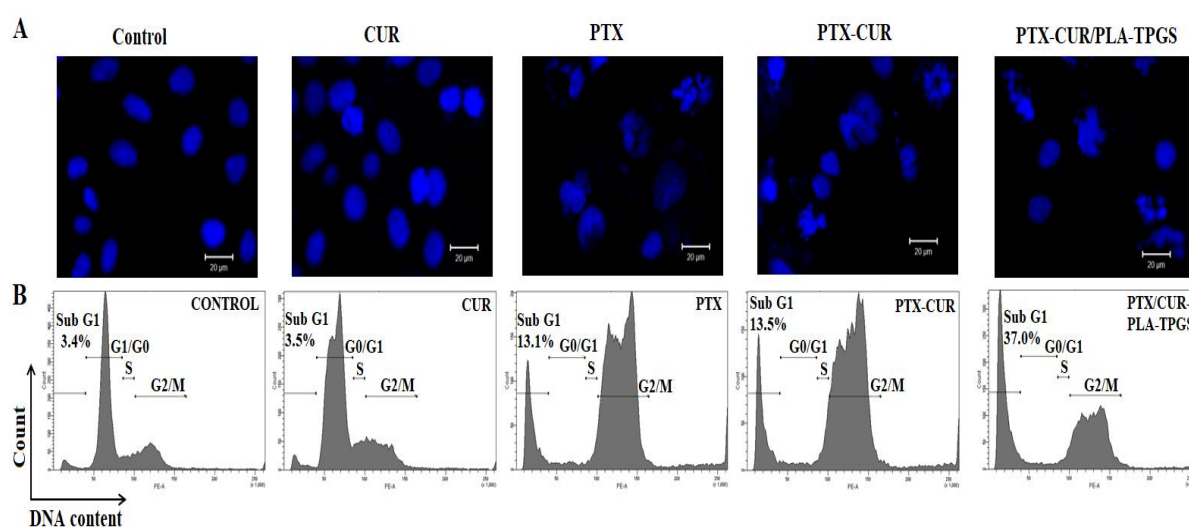


Figure 2. PTX-Cur/PLA-TPGS induced apoptosis in KPL4 cells. (A) Effect of PTX, Cur, PTX-Cur and PTX-Cur/PLA-TPGS at the same concentration (0.36 μM for paclitaxel and 1.68 μM for curcumin) for 48 hours on the cell cycle of KPL4 cells. (B) The immunofluorescence images expressed the morphology and size of nuclei in the cells treated with PTX, Cur, PTX-Cur and PTX-Cur/PLA-TPGS. (Cell nuclei were stained with Hoescht and observed on LSM 510).

Moreover, from day 3 of the treatment, the size of spheroids at all treated doses became smaller than the first day of treatment. Especially at the highest dose of 2.3 μM , there was a sharp decrease in the volumes of spheroids. In PTX-treated cells, the size of spheroids stayed unchanged and then started to increase from day 4 at the lower doses. The growth delay in PTX-treated cells was shorter than that of nanoparticles-treated cells. For example, at the lowest dose of 37 nM paclitaxel, the MCF7 spheroid growth delay was about one day when treated with PTX, but 4 days when treated with PTX-Cur/PLA-TPGS in comparison to the control. These results

indicated that PTX-Cur/PLA-TPGS not only inhibited the growth of the outer layer but also affected the second layer of spheroids - the layer consists of quiescent cells, and made the spheroid smaller. From the calculated volume of each spheroid treated with compounds, we defined the concentrations at which 50% inhibition of volume compared to the control at day 7 of treatment.

Figure 3B showed the dose-response curves of MCF7 spheroid volume under the effects of PTX and PTX-Cur/PLA-TPGS at day 7 of treatment with IC₅₀ of 1.108 $\mu\text{M} \pm 0.5$ and 40.013 $\mu\text{M} \pm 5.3$, respectively.

3.4. Curcumin in the Complex Plays the Second Function as the Label of Nanoparticles

Based on the autofluorescence of Curcumin, we checked the presence of PTX-Cur/PLA-TPGS when incubated with cells at concentration of $0.09 \mu\text{M}$ paclitaxel and $0.43 \mu\text{M}$ curcumin in 2 h, 4 h and 24 h. As shown in Figure 4, the level of PTX-Cur/PLA-TPGS increased in

KPL4 spheroid cells. The highest level was reached after 24 hours of incubation.

The nanoparticles concentrated in the cytoplasm of KPL4 cells around the nucleus. Using confocal laser scanning microscope, we found a significant difference in the distribution of nanoparticles inside the MCF7 spheroids with time.

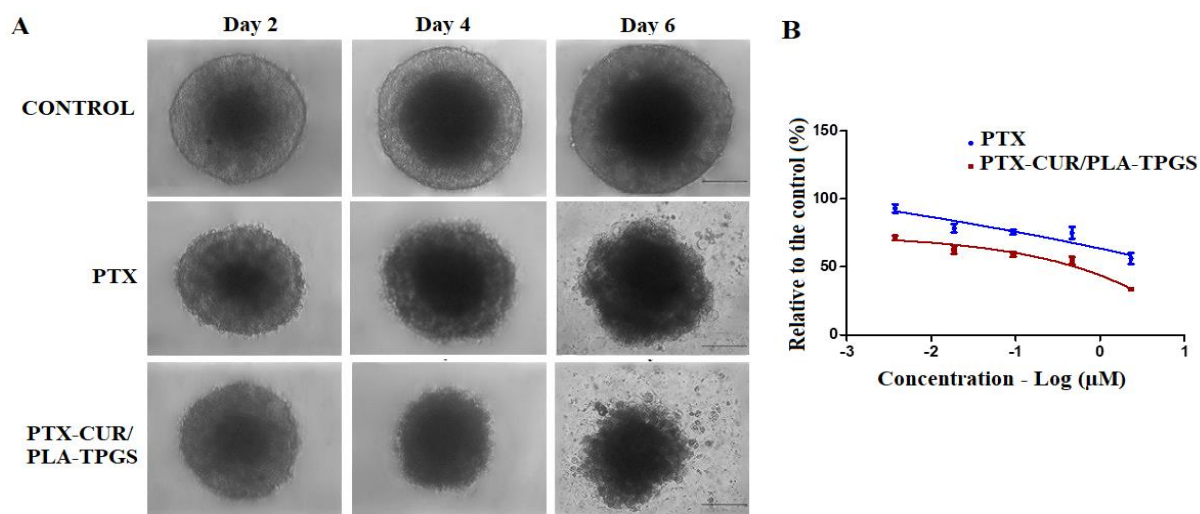


Figure 3. The effect of nanoparticles on the growth of MCF multicellular tumor spheroids.

(A) The morphology of MCF7 spheroids changed under the treatment with PT and PTX-Cur/PLA-TPGS at the concentration of $2.3 \mu\text{M}$ from day 2 to day 6 of treatment.

(B) Dose-response curve of MCF7 spheroid volume under the effects of PTX and PTX-Cur/PLA-TPGS after day 7 of treatment.

After 2 h, very little of the drugs stayed in cells of the outer layer of spheroids. At 4 h of incubation, there was an increase of fluorescence signal inside the spheroids. This signal decreased from outside to inside of spheroids. After 24 hours of incubation, the level of fluorescence signal increased and was distributed more deeply inside the spheroids. At the layer of $39 \mu\text{m}$ from the top of spheroid, and $200 \mu\text{m}$ from the side, the signal was still very strong. It is noted that the maximum diameter of spheroids normally reaches more than $1,000 \mu\text{m}$ with necrotic core larger than $400 - 500 \mu\text{m}$ [24]. Here, the mean diameter of spheroids used at the first day of this experiment is $370 - 400 \mu\text{m}$ (data not shown). It means that after 24 hours, PTX-Cur/PLA-TPGS successfully absorbed

through the outer layer and the quiescent cells layer and to the core of spheroids. Since the necrotic core of spheroids or tumor contains cells which have very high ability to metastasize [25], we propose that this more effective penetration may allow for better success in cancer treatment. These results also fit with our analysis of the ability of PTX-Cur/PLA-TPGS in attacking the second layer cells of the MCF7 spheroids.

Moreover, curcumin could be used as a very efficient tool in drug labeling. These results showed the potential of PTX-Cur/PLA-TPGS nanoparticles for applying in cancer theranostics. For that, these nanoparticles should be tested on in vivo model in the perspective works.

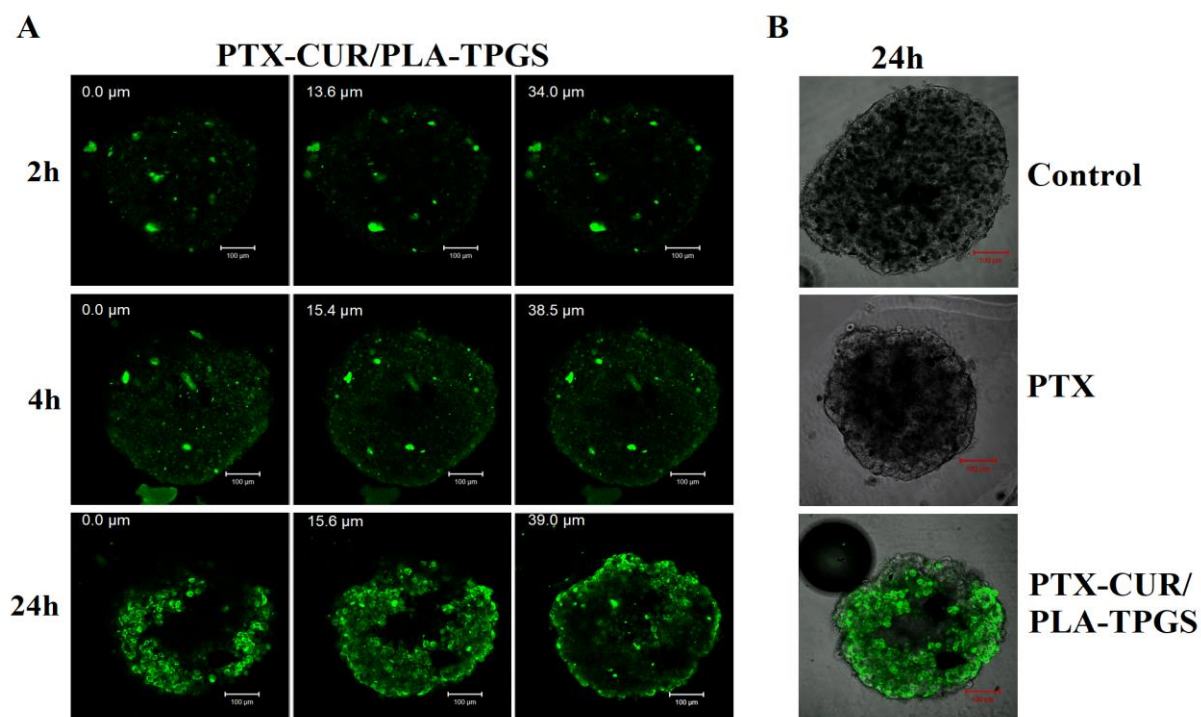


Figure 4. The absorption of PTX-Cur/PLA-TPGS into MCF7 spheroids can be visualized by the autofluorescence of Curumin in the nanoparticle complex. (A) Spheroids were incubated with drugs at a concentration of $0.09 \mu\text{M}$ paclitaxel and $0.43 \mu\text{M}$ curcumin. The images were taken after 2, 4 and 24 hours of incubation on LSM 510. The upper number on the left of each image represents the depth of the layer from the top to the bottom of the spheroid (i.e. the number is $0.0 \mu\text{m}$ means that it is the surface of the spheroid). (B) Fluorescence could not be detected in the control and PTX spheroids but presented in the PTX-Cur/PLA-TPGS one. The size of spheroids decreased when treating PTX and PTX-Cur/PLA-TPGS in comparison with the control.

4. Conclusion

We have successfully investigated and evaluated the bioactivity of (PTX combined Cur)-loaded PLA-TPGS nanoparticles. The combination of PTX and Cur in nanoparticles enhanced the inhibition of cell proliferation and also induced apoptosis in two breast cancer cell lines, MCF7 and KPL4, in comparison with PTX and Cur alone or the normal mixture of them. Moreover, PTX-Cur/PLA-TPGS showed very high ability in inhibiting MCF7-spheroids growth or even preventing the regrowth of the spheroids following the time of treatment. Interestingly, Cur in the combination could be used not only as the anti-tumor compound but also as an indicator of drug absorption.

Acknowledgements

The authors would like to thank Prof. Ross Fieldberg for critical reading.

References

- [1] H. Sung, J. Ferlay, R. L. Siegel, M. Laversanne, I. Soerjomataram, A. Jemal, F. Bray, Global Cancer Statistics 2020: GLOBOCAN Estimates of Incidence and Mortality Worldwide for 36 Cancers in 185 Countries, *CA Cancer J Clin*, Vol. 71, No. 3, 2021, pp. 209-249, <https://doi.org/10.3322/caac.21660>.
- [2] D. Gajria, A. Seidman, C. Dang, Adjuvant Taxanes: More to the Story, *Clin, Breast Cancer*, Vol. 10 Suppl 2, 2010, pp. 41-49, <http://doi.org/10.3816/CBC.2010.s.011>.

- [3] S. Lee, C. A. Schmitt, Chemotherapy Response and Resistance, *Curr, Opin, Genet, Dev*, Vol. 13, No. 1, 2003, pp. 6-90, [http://doi.org/10.1016/s0959-437x\(02\)00014-x](http://doi.org/10.1016/s0959-437x(02)00014-x).
- [4] J. D. Hurt, D. L. Richardson, L. G. Seamon, J. F. Fowler, L. J. Copeland, D. E. Cohn et al., Sustained Progression-free Survival with Weekly Paclitaxel and Bevacizumab in Recurrent Ovarian Cancer, *Gynecol, Oncol*, Vol. 115, No. 3, 2009, pp. 396-400, <https://doi.org/10.1016/j.ygyno.2009.08.032>.
- [5] B. Joe, M. Vijaykumar, B. R. Lokesh, Biological Properties of Curcumin-cellular and Molecular Mechanisms of Action, *Crit, Rev, Food Sci, Nutr*, Vol. 44, No. 2, 2004, pp. 97-111, <http://doi.org/10.1080/10408690490424702>.
- [6] H. P. Ammon, M. A. Wahl, Pharmacology of Curcuma Longa, *Planta, Med*, Vol. 57, No. 1, 1991, pp. 1-7, <http://doi.org/10.1055/s-2006-960004>.
- [7] B. B. Aggarwal, C. Sundaram, N. Malani, H. Ichikawa, Curcumin: the Indian Solid Gold, *Adv, Exp, Med, Biol*, Vol. 595, 2007, pp. 1-75, <http://doi.org/10.1007/978-0-387-46401-5-1>.
- [8] Q. Liu, W. T. Loo, S. C. Sze, Y. Tong, Curcumin Inhibits Cell Proliferation of MDA-MB-231 and BT-483 Breast Cancer Cells Mediated by Down-regulation of NF κ B, CyclinD and MMP-1 Transcription, *Phytomedicine*, Vol. 16, No. 10, 2009, pp. 916-922, <https://doi.org/10.1016/j.phymed.2009.04.008>.
- [9] A. Kunwar, A. Barik, B. Mishra, K. Rathinasamy, R. Pandey, K. I. Priyadarsini, Quantitative Cellular Uptake, Localization and Cytotoxicity of Curcumin in Normal and Tumor Cells, *Biochim, Biophys, Acta*, Vol. 1780, No. 4, 2008, pp. 673-679, <https://doi.org/10.1016/j.bbagen.2007.11.016>.
- [10] P. Anand, H. B. Nair, B. Sung, A. B. Kunnumakkara, V. R. Yadav, R. R. Tekmal et al., Design of Curcumin-loaded PLGA Nanoparticles Formulation with Enhanced Cellular Uptake, and Increased Bioactivity in Vitro and Superior Bioavailability in Vivo, *Biochem, Pharmacol*, Vol. 79, No. 3, 2010, pp. 330-338, <https://doi.org/10.1016/j.bcp.2009.09.003>.
- [11] Z. Zhang, S. S. Feng, Nanoparticles of poly(lactide)/vitamin E TPGS Copolymer for Cancer Chemotherapy: Synthesis, Formulation, Characterization and in Vitro Drug Release, *Biomaterials*, Vol. 27, No. 2, 2006, pp. 262-270, <https://doi.org/10.1016/j.biomaterials.2005.05.104>.
- [12] H. N. Nguyen, P. T. Ha, A. S. Nguyen, D. T. Nguyen, H. D. Do, T. Q. Nguyen, T. M. N. Hoang, Curcumin as Fluorescent Probe for Directly Monitoring in Vitro Uptake of Curcumin Combined Paclitaxel Loaded PLA-TPGS Nanoparticles, *Adv, Nat, Sci: Nanosci, Nanotechnol*, Vol. 7, 2016, pp. 025001, <https://doi.org/10.1088/2043-6262/7/2/025001>.
- [13] S. Ganta, M. Amiji, Coadministration of Paclitaxel and Curcumin in Nanoemulsion Formulations to Overcome Multidrug Resistance in Tumor Cells, *Mol, Pharm*, Vol. 6, No. 3, 2009, pp. 928-939, <https://doi.org/10.1021/mp800240j>.
- [14] L. Wei, C. Cai, J. Lin, T. Chen, Dual-drug Delivery System Based on Hydrogel/micelle Composites, *Biomaterials*, Vol. 30, No. 13, 2009, pp. 2606-2613, <https://doi.org/10.1016/j.biomaterials.2009.01.006>.
- [15] K. R. Kim, S. J. You, H. J. Kim, D. H. Yang, H. J. Chun, D. Lee, G. Khang, Theranostic Potential of Biodegradable Polymeric Nanoparticles with Paclitaxel and Curcumin Against Breast Carcinoma, *Biomater Sci*, Vol.9, No. 10, 2021, pp. 3750-3761, <http://doi.org/10.1039/d1bm00370d>.
- [16] P. T. Ha, T. M. N. Tran, H. D. Pham, Q. H. Nguyen, X. P. Nguyen, The Synthesis of Poly (Lactide)-vitamin E TPGS (PLA-TPGS) Copolymer and Its Utilization to Formulate a Curcumin Nanocarrier, *Adv, Nat, Sci: Nanosci, Nanotechnol*, Vol. 1, No. 1, 2012, pp. 7, <https://doi.org/10.1088/2043-6254/1/1/015012>.
- [17] C. Riccardi, I. Nicoletti, Analysis of Apoptosis by Propidium Iodide Staining and Flow Cytometry, *Nat, Protoc*, Vol. 1, 2006, pp. 1458-1461, <https://doi.org/10.1038/nprot.2006.238>.
- [18] J. M. Kelm, N. E. Timmins, C. J. Brown, M. Fussenegger, L. K. Nielsen, Method for Generation of Homogeneous Multicellular Tumor Spheroids Applicable to a Wide Variety of Cell Types, *Biotechnol, Bioeng*, Vol. 83, No. 2, 2003, pp. 173-180, <https://doi.org/10.1002/bit.10655>.
- [19] M. Vinci, S. Gowan, F. Boxall, L. Patterson, M. Zimmermann, W. Court et al., Advances in Establishment and Analysis of Three-dimensional Tumor Spheroid-based Functional Assays for Target Validation and Drug Evaluation, *BMC, Biol*, Vol. 10, 2012, pp. 29, <https://doi.org/10.1186/1741-7007-10-29>.
- [20] S. V. Bava, V. T. Puliappadamba, A. Deepti, A. Nair, D. Karunakaran, R. J. Anto, Sensitization of Taxol-induced Apoptosis by Curcumin Involves Down-regulation of Nuclear Factor-kappaB and the Serine/threonine Kinase Akt and is Independent of Tubulin

- Polymerization, *J. Biol, Chem*, Vol. 80, No. 8, 2005, pp. 6301-6308,
<https://doi.org/10.1074/jbc.M410647200>.
- [21] V. L. Galic, J. D. Wright, S. N. Lewin, T. J. Herzog, Paclitaxel Poliglumex for Ovarian Cancer, *Expert, Opin, Investig, Drugs*, Vol. 20, No. 6, 2011, pp. 13-21,
<https://doi.org/10.1517/13543784.2011.576666>.
- [22] M. T. Silva, A. D. Vale, N. M. D. Santos, Secondary Necrosis in Multicellular Animals: an Outcome of Apoptosis with Pathogenic Implications, *Apoptosis*, Vol. 13, 2008, pp. 463-482,
<https://doi.org/10.1007/s10495-008-0187-8>.
- [23] M. V. Blagosklonny, Mitotic Arrest and Cell Fate: Why and How Mitotic Inhibition of Transcription Drives Mutually Exclusive Events, *Cell Cycle*, Vol. 6, No. 1, 2007, pp.70-74,
<https://doi.org/10.4161/cc.6.1.3682>.
- [24] L. A. K. Schughart, J. P. Freyer, F. Hofstaedter, R. Ebner, The Use of 3-D Cultures for High-throughput Screening: the Multicellular Spheroid Model, *J. Biomol, Screen*, 2004, pp. 273-285,
<https://doi.org/10.1177/1087057104265040>.
- [25] M. R. Choi, K. J. Stanton-Maxey, J. K. Stanley, C. S. Levin, R. Bardhan, D. Akin et al., A Cellular Trojan Horse for Delivery of Therapeutic Nanoparticles into Tumors, *Nano, Lett*, Vol. 7, No. 12, 2007, pp. 3759-3765,
<http://doi.org/10.1021/nl072209>.